RESEARCH ARTICLE



Check for updates

Influence of groundwater and topography on stream drying in semi-arid headwater streams

Sara R. Warix¹ | Sarah E. Godsey¹ | Kathleen A. Lohse^{1,2} | Rebecca L. Hale²

Correspondence

Sara R. Warix, Hydrologic Science and Engineering, Colorado School of Mines, Golden, Colorado, 80401, USA Email: swarix@mymail.mines.edu

Funding information

USDA-Agricultural Research Service, Grant/ Award Numbers: 1331872, 1653998

Abstract

Non-perennial streams comprise over half of the global stream network and impact downstream water quality. Although aridity is a primary driver of stream drying globally, surface flow permanence varies spatially and temporally within many headwater streams, suggesting that these complex drying patterns may be driven by topographic and subsurface factors. Indeed, these factors affect shallow groundwater flows in perennial systems, but there has been only limited characterisation of shallow groundwater residence times and groundwater contributions to intermittent streams. Here, we asked how groundwater residence times, shallow groundwater contributions to streamflow, and topography interact to control stream drying in headwater streams. We evaluated this overarching question in eight semi-arid headwater catchments based on surface flow observations during the low-flow period, coupled with tracer-based groundwater residence times. For one headwater catchment, we analysed stream drying during the seasonal flow recession and rewetting period using a sensor network that was interspersed between groundwater monitoring locations, and linked drying patterns to groundwater inputs and topography. We found a poor relationship between groundwater residence times and flowing network extent $(R^2 < 0.24)$. Although groundwater residence times indicated that old groundwater was present in all headwater streams, surface drying also occurred in each of them, suggesting old, deep flowpaths are insufficient to sustain surface flows. Indeed, the timing of stream drying at any given point typically coincided with a decrease in the contribution from near-surface sources and an increased relative contribution of groundwater to streamflow at that location, whereas the spatial pattern of drying within the stream network typically correlated with locations where groundwater inputs were most seasonally variable. Topographic metrics only explained ~30% of the variability in seasonal flow permanence, and surprisingly, we found no correlation with seasonal drying and down-valley subsurface storage area. Because we found complex spatial patterns, future studies should pair dense spatial observations of subsurface properties, such as hydraulic conductivity and transmissivity, to observations of seasonal flow permanence.

KEYWORDS

groundwater, groundwater residence time, intermittent streams, topography

¹Department of Geosciences, Idaho State University, Pocatello, Idaho, USA

²Department of Biological Sciences, Idaho State University, Pocatello, Idaho, USA

1 | INTRODUCTION

Steep mountain streams continue to flow long after their seasonal snowpacks have melted and no rain has fallen for weeks or months because flow is often sustained by groundwater contributions (Carroll et al., 2018; Freeze, 1974; Frisbee et al., 2017; Godsey et al., 2013; Rumsey et al., 2015; Segura et al., 2019). However, these groundwater contributions may fail to sustain streamflow when evapotranspiration (ET) demands are high, or when subsurface transmissivity (slope, cross-sectional area, and conductivity) is high (Prancevic & Kirchner, 2019). Groundwater sources include both shallow and deep flowpaths through soil and bedrock (Frisbee et al., 2011), but partitioning these sources is complicated by interactions between spatially heterogeneous and dynamic surface and subsurface processes (Fleckenstein et al., 2006; Ghosh et al., 2016; Kirchner, 2009; McDonnell et al., 2007; Radke et al., 2019). Spatiotemporally variable groundwater inputs will likely become more important to understanding water resources as climate changes, especially in mountainous headwaters of the western U.S., where snowpack is predicted to decline and precipitation mostly falls in winter (Earman & Dettinger, 2011; Klos et al., 2014; Lundquist et al., 2009; Mote et al., 2018; Nolin & Daly, 2006; Segura et al., 2019). The projected decreases in surface storage in snowpack will potentially increase the importance of subsurface storage in sustaining surface flows (Tague & Grant. 2009).

Surface flows are commonly characterised as perennial or nonperennial based on whether they dry during typical years (Busch et al., 2020). Non-perennial streams include both ephemeral streams that flow only in response to precipitation events and intermittent streams that flow seasonally. Intermittent streams often disconnect from the water table during dry months, sometimes forming isolated pools (Busch et al., 2020). Approximately 59% of the streams in the United States are non-perennial, with ~80% drying in arid and semiarid regions, and such streams are also commonly the headwaters of larger streams and rivers (Gutiérrez-Jurado et al., 2019; Levick et al., 2008). During the last two decades, our understanding of stream drying patterns and their controls has improved (e.g., Costigan et al., 2016; Godsey & Kirchner, 2014; Gutiérrez-Jurado et al., 2019; Prancevic & Kirchner, 2019; Zimmer & McGlynn, 2017a), and the multiscale processes in meteorology, geology, and land cover that govern stream drying have been recognised (Costigan et al., 2016; Jaeger et al., 2019). For example, climatic controls often dominate at a continental scale (e.g., Eng et al., 2015), but within a catchment, topography dictates where flow accumulates and thus modulates the subsurface-to-surface transition of flow within channel networks (Prancevic & Kirchner, 2019). Because topographic metrics are relatively easy to calculate, predicting stream drying from them is appealing, although other factors may drive local or even regional drying patterns. Perennial and intermittent flow is sourced by a variety of subsurface flowpaths (Dohman, 2018) and the depth of channel fill and underlying lithology can impact the local accumulation of surface flow (Lovill et al., 2018). In addition, water can accumulate where soil stratigraphy allows for the development of perched water tables

(Zimmer & McGlynn, 2017a), as dictated by soil type (Gutiérrez-Jurado et al., 2019). Despite these advances, the spatial pattern and timing of stream drying cannot yet be reliably predicted within a catchment, because of both poor characterisation of how groundwater influences drying at different spatial and temporal scales, and our limited understanding of the processes that govern the coupling between groundwater and stream drying.

Stable groundwater contributions to surface water should facilitate perennial flows. At local to regional scales, groundwater flow may be strongly influenced by subsurface transmissivity and flowpath lengths, which will in turn determine groundwater residence times. Groundwater residence times vary throughout catchments (Burns et al., 2003; Kolbe et al., 2016; Manning et al., 2012; Rademacher et al., 2001), and vary predictably with mean hydraulic conductivity (Hale & McDonnell, 2016; Maxwell et al., 2015). Thus, variation in subsurface transmissivity along the stream corridor, and/or variation in flowpath length and recharge location, could lead to spatial variation in streamflow permanence that may be related to groundwater residence times. Groundwater residence times, an integrated measure of subsurface transmissivity, are most readily measured at springs. Because resilient springs exist where groundwater has long flowpaths (Erman & Erman, 1995), and longer flowpaths often result in longer residence times (Manning et al., 2012), it is possible that stream flow permanence below those springs would also vary with groundwater residence time. Groundwater with long residence times is often a major contributor to streamflow, although there usually are multiple flowpaths sustaining streamflow (Frisbee et al., 2011). If those other flowpaths dominate, and especially if the local conditions that cause a spring to emerge at the surface differ from the conditions driving more diffuse groundwater contributions, there may be no predictable relationship with downstream flow permanence. Thus, assessing how groundwater residence times and contributions at springs and along more diffuse groundwater flowpaths affect intermittent stream networks deserves more attention.

Diffuse groundwater contributions to streams vary throughout a stream network (Partington et al., 2012; Payn et al., 2012; Rumsey et al., 2015; Segura et al., 2019) and may contribute to spatiotemporal stream drying patterns. Our current understanding of these more diffuse groundwater contributions stems mostly from perennial streams and rivers (but see Zimmer & McGlynn, 2017a, 2017b). In this paper, we define runoff as surface or near-surface waters with low specific conductivity that contribute to streamflow (following Miller et al., 2014) and we define groundwater as an integrated signal from all deeper subsurface waters with high specific conductivity values entering the stream (sensu Hall, 1968 and Miller et al., 2014). Hydrograph separation techniques can be used to partition "runoff" and "baseflow," or groundwater contributions (e.g., Carey et al., 2013; Hall, 1968; Liu et al., 2013; Miller et al., 2014). Although hydrograph separation techniques have been successfully applied to perennial rivers, their application to intermittent streams remains limited (Zimmer & McGlynn, 2018), and may help identify linkages between groundwater contributions and stream drying. One key hydrograph separation approach relies on electrical conductivity measurements of

potential sources of water to streams (Laudon et al., 2004; Matsubayashi et al., 1993; Pellerin et al., 2008), such as groundwater and near-surface flows (Maurya et al., 2011; Penna et al., 2014). Other hydrograph separation techniques utilise stable isotopes or more detailed hydrochemistry, and can lead to different separation results, especially when they identify more sources than conductivity-based separations (Hooper & Shoemaker, 1986; Klaus & McDonnell, 2013). However, because conductivity can be relatively easily measured continuously throughout a network, they can be helpful for understanding fine-scale spatiotemporal variations in contributions.

Topography, especially in mountainous headwater catchments, may also affect groundwater contributions and control spatiotemporal patterns of low flows (Welch et al., 2012). Topography directly affects the hydraulic head that drives groundwater flows, and may indirectly reflect the depth of weathered bedrock, controlling flowpath lengths (Clair et al., 2015); indeed curvature, contributing area, topographic wetness index, and transmissivity have been used to explain drying patterns (Prancevic & Kirchner, 2019; Whiting & Godsey, 2016). However, local topography only explains some of the local spatial variation in flow duration along a stream network (Jensen et al., 2019), indicating other factors also influence flow permanence. For example, landslide deposits or small sediment accumulation behind downed trees temporarily caught in the channel network may affect local transmissivity over relatively short timescales (Godsev & Kirchner, 2014: Lovill et al., 2018). Transmissivity affects how subsurface water travels through porous media in the stream corridor, and depends on down-valley subsurface storage capacity, which varies along the length of a headwater stream (Ward et al., 2018). However, unlike topographic metrics, subsurface characteristics are challenging to measure. Despite catchment-scale connections between topography and stream drving, it remains unknown whether local stream drving is driven more by topography, subsurface geometry and storage, or other flow controls such as heterogeneity in hydraulic conductivity.

Here, we combine network-scale snapshots of stream drying and groundwater residence times with a local-scale geomorphic assessment. We also relate high-frequency observations of drying patterns to groundwater inputs in headwater streams. We ask: (1) How do groundwater residence times vary with surface flow permanence at the catchment scale?, (2) How are groundwater inputs and stream drying related over space and time?, and (3) How well can topographic metrics predict local variability in stream drying? We hypothesise that longer groundwater residence times will yield greater surface flow permanence, stable groundwater inputs will ensure surface flow permanence, and that topographic metrics and subsurface geometry will be good predictors of flow permanence.

2 | SITE DESCRIPTION AND STUDY DESIGN

2.1 | Study design

We quantified spatiotemporal patterns of stream drying based on observations at specific locations in space and moments in time, and then integrated these observations throughout the network and over the entire observation period. To answer question 1, we mapped the extent of surface flow in eight sub-catchments within the Reynolds Creek Experimental Watershed and Critical Zone Observatory (RC CZO) and collected spring samples for CFC analysis from six of the eight streams to quantify groundwater residence times. To further elucidate the relationship between shallow groundwater and stream drying (question 2), we focused on one stream, Murphy Creek, where we made distributed observations of stream drying and collected stream stage and groundwater data. Finally, to assess whether topographic metrics can be used to predict the probability of stream drying (question 3), we compared local topographic metrics and subsurface geometry within Murphy Creek to spatiotemporal drying patterns.

2.2 | Site description

The RC CZO is a 239-km² semi-arid catchment located in southwestern Idaho (Sevfried et al., 2018) that is snow-dominated at higher elevations and rain-dominated at lower elevations. It consists of 13 instrumented sub-catchments that contribute to the larger Revnolds Creek, which eventually flows into the Snake River (Pierson et al., 2000). Eight of the headwater streams in RC CZO-Babbington Creek, Cottle Creek, Macks Creek, Murphy Creek, Dryden Creek, the north fork of Peter's Gulch, the south fork of Peter's Gulch, and Revnolds Mountain East (RME) Creek (Figure 1)—have a spring adjacent to the stream suitable for chlorofluorocarbon (CFC) dating of groundwater (based on initial surveys in October 2018); however, only six of these eight springs were sampled in August 2019 because flows had decreased substantially at two springs, increasing atmospheric exchange and therefore leading to unrepresentative CFC ages (see Section 3.2.1 for details). All springs flowed directly into the stream, except for the spring adjacent to the south fork of Peter's Gulch where spring flows infiltrate back into the subsurface.

We focused on one catchment, Murphy Creek, to study the influence of groundwater inputs after previous observations indicated potentially complex stream drying patterns (MacNeille et al., 2020). Murphy Creek (1.29 km², 1598 m mean elevation) has a \sim 2.5-km channel (Figure 1) and receives a mean annual precipitation of 639 mm/yr (Kormos et al., 2016). RC CZO precipitation for the 2019 water year was 128% of normal based on data from 1963-2019 collected by the Agricultural Research Station in nearby Tollgate watershed (station 116) that drains a wider range of elevations than Murphy (Center, U. A. N. W. R., 2020; more information about Tollgate can be found in Pierson et al., 2000). The snowpack is not measured continuously at Murphy, but in 2019, the snowpack was \sim 129% of the long-term average (1999–2019) at the higher-elevation RME catchment (Center, U. A. N. W. R., 2020). The rain/snow partitioning in Murphy Creek is approximately similar to that at the ARS long-term weather station 127, which is at a similar elevation though about 15 km to the SE; snow typically comprises 45% of the annual precipitation at weather station 127 (Nayak et al., 2010). Unfortunately, spatially distributed rain-snow partitioning was not available for Murphy Creek in for 2019. The Murphy Creek basin is underlain

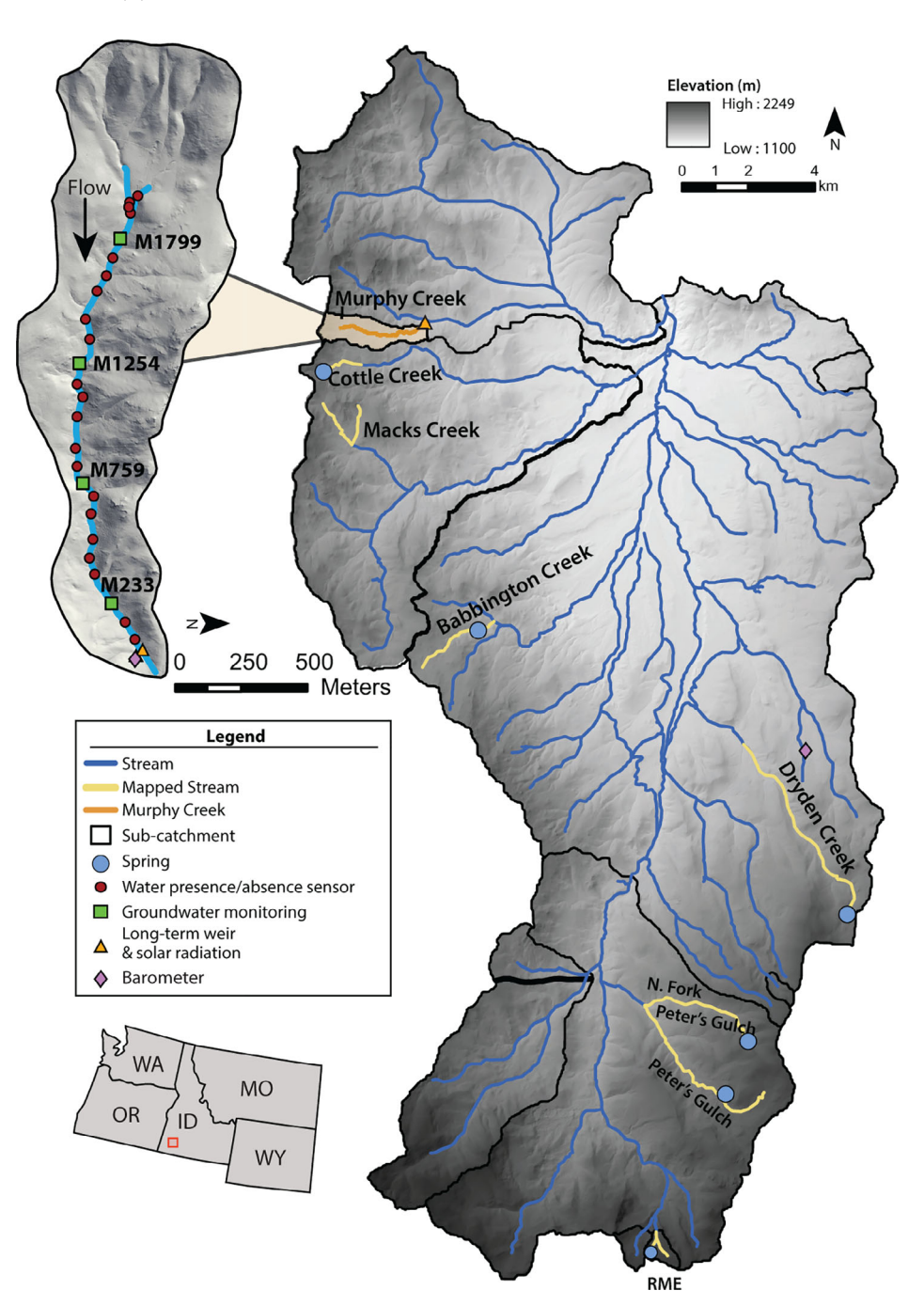


FIGURE 1 Reynolds Creek Critical Zone Observatory with sub-catchment Murphy Creek highlighted in orange. In the zoomed-in map of Murphy Creek, the locations of monitoring equipment are shown (Table S1 in Data S1). Red circles show sensors measuring the presence or absence of water and green squares indicate where groundwater inputs are quantified with EC and water-level sensors. In the larger RC CZO map, streams shown in yellow were mapped once on August 5-6, 2019. Springs sampled for CFCs are indicated by blue circles; springs also exist in Macks and Murphy Creek, but were not suitable for CFC sampling when the mapping took place

by Salmon Creek volcanics (56%) and Reynolds Basin basalt and latite (44%). In 2015, the Soda Fire burned the Murphy catchment, but the basin's functions largely recovered from the fire within 2 years (Vega et al., 2020).

3 | METHODS

3.1 | Drying terminology

In this analysis, we adopt integrated metrics based on observations of the presence or absence of flow at a given sensor location at a

given moment in time (Table 1). Seasonal flow permanence summarises temporal variation in flow at a single location and is calculated as the fraction of the observation period with surface flow at a given location. Instantaneous flowing network extent summarises spatial variation in surface flow across the network at a single point in time and is calculated as the percent of sensor locations (or mapped reaches) that are flowing at a given moment. Seasonal flowing network extent integrates over both time and space and summarises the spatiotemporal patterns of surface flow across the stream network and observation period; it is calculated as the percent of sensor locations with surface flow integrated over the observation period.

TABLE 1 Terminology and metrics used to discuss spatial, temporal, and spatiotemporal patterns of stream drying at a point and throughout the network, both at any given moment in time and throughout the season (in this case, the full observation period from April through October)

	Spatiotemporal metrics			
	Moment	Season		
Point	Presence/absence of flow [flow/no flow]	Seasonal flow permanence [% of season with flow at a given location]		
Network	Instantaneous flowing network extent [% of sensors flowing or % of mapped stream flowing at a given moment]	Seasonal flowing network extent [% of sensors flowing integrated across season]		

Note: At Murphy Creek, 21 presence/absence sensors and four groundwater monitoring locations generated the data used to calculate the metrics, leading to a maximum total of 25 sensors for any given metric. The instantaneous flowing network extent for the eight mapped catchments (Figure 2) is calculated as a percent of the entire mapped headwater channel network. In each quadrant of the table, the bold term is listed with a definition of the term directly below in brackets.

3.2 | Stream mapping and groundwater residence times

The instantaneous flowing network extent (Table 1) was mapped once in eight headwater streams at RC CZO (Figure 2) in late summer 2019 to evaluate the relationship between groundwater residence times and surface flow permanence during low-flow periods. All streams were mapped on August 5 or 6, 2019 when flows at the nearby Tollgate catchment located at the outlet of the RC CZO were 16% of the long-term average (1963-2019) (Center, U. A. N. W. R., 2020). Two individuals mapped each stream using ESRI collector installed on Samsung Galaxy Tablets with GPS and GLONASS (2-5 m accuracy). One individual walked stream-right while the other walked stream-left so that no branching or tributaries were missed; stream branches were mapped until flow ceased. (Note that the south fork of Peter's Gulch contained several small tributaries that were not mapped due to logistic constraints). Isolated wet or dry segments shorter than 3 m long were not included in the mapping. We marked flow start and stop points using ESRI Collector, and delineated flowing and dry segments between marked points based on LiDAR-delineated channels. We primarily focused on first-order headwater streams with adjacent rheocrene springs (Springer & Stevens, 2009).

3.2.1 | Spring sampling and analyses

At six of the eight headwater streams (Figures 1 and 2), a spring adjacent and flowing into the stream channel was sampled for CFC-11 and CFC-12. All springs contributed to surface flows in the

stream, but were not the only source of flow. Springs at Murphy Creek and Macks Creek were not suitable for CFC analysis because very low flow rates prevented the collection of uncontaminated samples. CFC samples were collected in triplicate in 500-ml glass bottles at the spring source or uppermost discharge location before being sealed with foil caps and electrical tape following methods suggested by the University of Miami Tritium Laboratory (detailed in SI.6 in Data S1), where samples were analysed (https://tritium.rsmas.miami.edu/analytical-services/advice-on-sampling/cfc-and-sf6/index.html).

To calculate residence times for each spring, we had to assume a recharge temperature (mean RC CZO temperature during Oct-May recharge season) and elevation (watershed divide elevation). For all springs, except for the highest-elevation spring in RME (RSS3), we assumed a recharge elevation of 1650 m and a recharge temperature of 4°C, which is the average air temperature during the months with the most precipitation (October-April) at Murphy Creek. For the highest-elevation spring, we assumed a recharge elevation of 2100 m and a recharge temperature similar to the average air temperature during the months with the most precipitation (October-April) of 0°C. CFC ages were calculated using the USGS's CFC evaluation spreadsheet program (https://water.usgs.gov/lab/software/USGS_CFC/), derived from Plummer et al. (2006). Reported ages have an error of ±2 years based on analytical uncertainty reported by the lab. The sensitivity of the results to the recharge elevation was tested for a plausible elevation range between 1650 and 2100 m, and the resulting age change was insignificant (<1 year). In addition, we tested sensitivity to recharge temperature between 0-8°C; the resulting age calculations had a 9-year range.

3.3 | Murphy Creek surface flow presence and groundwater inputs

We determined stream specific conductivity (SC) and water level at four locations in Murphy Creek to determine groundwater inputs, using two-endmember hydrograph separation with SC as a tracer (Miller et al., 2014; Pellerin et al., 2008). Because of our study focus at these sites, we refer to these four sites as "groundwater monitoring locations"; they were $\sim\!500$ m apart, and from lowest to highest elevation had the following upstream contributing areas: 1.04, 0.87, 0.69, 0.34 km². We measured SC with HOBO electrical conductivity dataloggers (Onset Hobologger, U-24) and the water level with HOBO water-level dataloggers (Onset Hobologger, U-20). Water-level and electrical conductivity sensors were housed in black 2" Polyvinyl chloride (PVC) that was slightly longer than the length of the sensor and contained holes so that water could freely enter and exit the pipe at the stream bed interface.

A Vaisala HMP155 humidity and temperature probe was used to determine air temperature and a LI-7500RS Open Path $\rm CO_2/H_2O$ Analyser to measure the barometric pressure every 30 min. Specific conductivity was calculated as electrical conductivity at 25°C (USGS, 2019). Quality assurance and control corrections to maintain

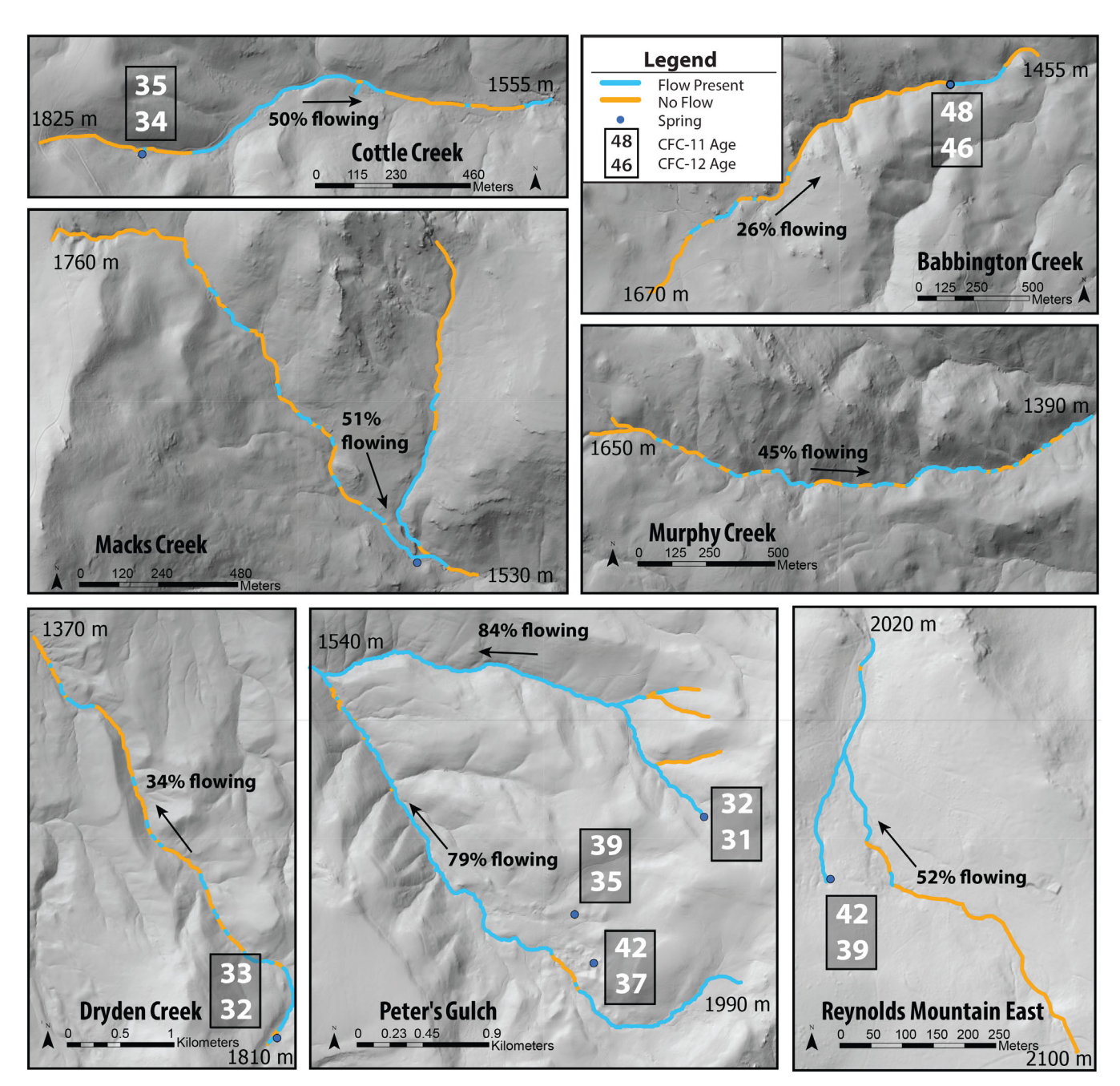


FIGURE 2 Stream flow mapping results for Babbington Creek, Cottle Creek, Dryden Creek, Macks Creek, Murphy Creek, and Peter's Gulch, where blue indicates the presence of surface flow and orange indicates a dry channel. Locations of streams within the Reynolds Creek catchment are shown in Figure 1. All streams were mapped on August 5–6, 2019 (Table S3 in Data S1). Calculated residence times (in years) for CFC-11 and CFC-12 are displayed in boxes adjacent to each spring: the CFC-11 age is printed above the CFC-12 age (also see Table S4 in Data S1). Springs in Macks and Murphy Creeks were unsuitable for CFC sampling at the time of mapping, and thus no ages are reported. An arrow shows the flow direction in each stream and is labelled with the instantaneous flowing network extent, expressed as a percentage of the mapped channel network

high-quality specific conductivity measurements are detailed in supplementary information (Section SI.2 in Data S1).

We detected water presence and absence with modified HOBO Pendant Loggers (Onset HOBO Pendant/Light 64 K Datalogger UA-002-64) at 21 locations in Murphy Creek. The Pendant/Light 64 K Dataloggers were modified following methods from Chapin et al. (2014). Pendants were housed in grey PVC pipe and installed so

that the two pole electrodes at the bottom of the plastic housing were in constant contact with the stream bed and thus were able to detect the lowest of flows. Pendants were located at the deepest part of the channel, typically in pools below steps (see SI.3 in Data S1). The four EC data loggers were also used to detect water presence, however these sensors could not detect water below 1.6 cm (the combined height of the housing and distance to the sensor), so very low flows

were not captured. In total, there were 25 presence/absence measurement locations, with $\sim\!80$ m between each sensor. Each of these 25 sensors is hereby referred to as sensor #MX, where X is the distance in metres from the outlet weir.

All sensors recorded data at 15-minute intervals from June 3 to October 1, 2019. Sensors were visited during the weeks of June 3, June 10, July 7, August 5, September 9, and October 1, 2019. Seven of the Pendant sensors were added on July 10, 2019 (M454, M716, M823, M1121, M1377, M1653, and M1951). For these seven sensors, we made several assumptions about flow conditions between June 3 and July 10. Flow was observed at all sites during field visits from June 3-12, and all seven stream locations were assumed to be flowing during this period. From June 12-July 10, we assumed continuous flow only if flow was observed the entire week after installation on 10 July (M454, M716, M1377, M1653, and M1951). For the two remaining sensors (M823, M1121), gaps in flow were observed between July 10 and July 17, and we made no assumptions about whether the stream was flowing or dry between June 12 and July 10. Other gaps in flow presence records were due to logger failure (M1166, M1653, M1799).

3.3.1 | Surface and groundwater calculations

Water-level calculations

We determined stream water levels by subtracting barometric pressure from in-stream pressure readings. Because in-stream water-level pressure was collected every 15 min, and barometric pressure and air temperature were only collected every 30 min, simple linear interpolation was used to estimate the missing air temperature and pressure values. Barometric pressure readings collected at Nancy's Gulch, a sub-catchment \sim 13 km southeast of Murphy Creek at a similar elevation (Nancy's Gulch Meteorological Station: 1426 m, Murphy Creek Weir: 1392 m; Figure 1), were corrected to the elevation of each instream water-level logger for all pressure measurements (detailed in the SI.1 in Data S1).

Stage-discharge relationship

We assumed a power-law stage-discharge relationship ($Q=aZ^b$), where a and b are constants, and Z is the barometric pressure-corrected stage height or water level (cm), to calculate discharge at 15-minute intervals throughout the observation period. Discharge was measured three to six times at each groundwater monitoring location using the salt dilution method (Moore, 2003) (Figure S3 and Table S2 in Data S1). At location M759, discharge was only measured three times because of early and sustained drying. At M1254, extrapolation of our limited stage-discharge observations (N=6) to high stage values at the beginning of the observation period generated physically implausible discharge estimates. Thus, for all stages above 10 cm, we relied on qualitative in-field observations and adjusted the stage-discharge relationship by assuming 15 cm was equal to 25 L/s. We propagated measurement uncertainty to every discharge calculation: errors were large (100–200% of the reported value) because our

primary focus was on low-flow periods where water levels are low and pressures differ only slightly from barometric pressure. Nonetheless, we have confidence in the relative discharge values because of our repeated field observations.

Groundwater contributions

Discharge and SC measurements were combined to calculate the groundwater component of the hydrograph for each 15-minute timestep using Equation 1 (Miller et al., 2014):

$$Q_{GW} = Q \frac{[SC - SC_{RO}]}{[SC_{GW} - SC_{RO}]}$$
 (1)

where Q_{GW} is the groundwater flow (L/s) at time t, Q is the total discharge (L/s) at time t, SC is the specific conductivity (μ S/cm) measured at time t, SC_{RO} is the specific conductivity of the runoff endmember, and SC_{GW} is the specific conductivity of the groundwater end-member. Each monitoring location was assigned a unique groundwater and runoff endmember. The runoff endmember represents the low-SC water that is delivered to the stream from surface or shallow nearsurface inputs, such as snowmelt or rainfall; it was assumed to be similar to the average upstream SC in March (MacNeille, personal comm.; see details in SI.4 in Data S1). This streamflow in March likely has a groundwater component as groundwater still contributes to discharge during peak flows, but we assume that this component is small and that the SC at this time largely reflects the surface and near-surface components. The groundwater end-member was assumed to be the maximum observed SC in the stream over the period of record because no wells were available within the watershed to determine the groundwater SC or its dynamics. For each site, the maximum SC was similar to observed spring and groundwater SC values within the larger Reynolds Creek watershed (Souza, pers. comm.). The percent groundwater in streamflow was determined by dividing the groundwater (Q_{GW}) by the total discharge (Q) at the same timestep. If no flow was observed, percent groundwater was assigned 100% under the assumption that groundwater was present in the subsurface.

3.4 | Topographic metrics and stream drying

We calculated local topographic metrics for the Murphy Creek watershed using an 1-m DEM derived from LiDAR (Ilangakoon et al., 2016) to determine whether they predict stream drying variability. The upslope contributing area, profile curvature, and local slope were computed for all points within the Murphy catchment using TopoToolbox 2, a MATLAB-based toolbox for topographic analysis (Schwanghart & Scherler, 2014). The topographic attributes were extracted for all sensor locations by snapping the sensor locations determined in the field with the GPS to the nearest delineated stream. The topographic wetness index (TWI) was also calculated for each sensor location (Beven & Kirkby, 1979) as TWI is a topographic metric commonly used to quantify topographic controls on hydrologic process (Sørensen et al., 2006). All metrics were plotted against the

seasonal flow permanence (Table 1) for each sensor location to assess geomorphic controls on drying patterns.

We also estimated the down-valley subsurface storage area at each sensor location in Murphy Creek similar to Ward et al. (2018). We identified a likely stream corridor based on the extracted topographic profile at each cross-section and field observations. Unlike Ward et al. (2018), we did not assume that the stream corridor depth was constant, and instead assumed that the subsurface profile was Vshaped due to extensive fluvial erosion in the stream corridor topped with variable amounts of valley fill (Vega et al., 2020). To estimate the amount of fill, we extracted topographic profiles (z(x)) perpendicular to the stream at each of the sensor locations and found the minimum elevation in the cross-sectional profile at the thalweg of the stream (point T in Figure S2 in Data S1). The maximum valley width, w, varied between 5 and 50 m. We then used this width to define points A and D, at locations T-w and T+w, respectively, and searched between A and D to identify the points on each hillslope with the largest change in slope on each side of point T, which was assumed to indicate the transition from the hillslope to valley fill (points B and C in Figure S2 in Data S1). We then fit a line to all points above each break in slope (red dashed lines between points A and B or between points C and D in Figure S2 in Data S1), and projected these hillslope profiles below the observed topography until they intersected, to generate the assumed V-shaped valley cross-sectional profile. The difference between this assumed V-shaped valley profile and the actual topographic profile is assumed to represent the area through which downvalley subsurface water can flow (hatched area in Figure S2 in Data S1). If the projected lines plotted above the topographic profile, the subsurface storage area at that point was set to zero (see red dashed line above the topographic profile for a portion of the projection between points B and T in Figure S2 in Data S1). More details of the calculation are given in supplementary information (Section SI.5 in Data S1). Limitations of this approach and methods to test its assumptions are discussed in Section 5.3.

4 | RESULTS

4.1 | Stream mapping and groundwater residence time

The instantaneous flowing network extent ranged from 16% to 74% of the entire stream network for the eight headwater streams that we mapped within the RC CZO on August 5–6, 2019 (Figure 2 and Table S3 in Data S1). Instantaneous flow was more continuous in some streams than others. There were long flowing and dry segments in Babbington Creek, Cottle Creek, RME, and Peter's Gulch; in contrast, Dryden Creek, Macks Creek, and Murphy Creek had many short flowing and dry segments. Groundwater residence times from the six springs suitable for CFC sampling ranged from 32–48 ±2 years based on CFC-11 and 31–46 ±2 years based on CFC-12 (Figure 3 and Table S4 in Data S1). Despite the variation in drying patterns in these catchments, and in contrast to our hypothesis, groundwater residence time based on the CFC samples from springs adjacent to each stream

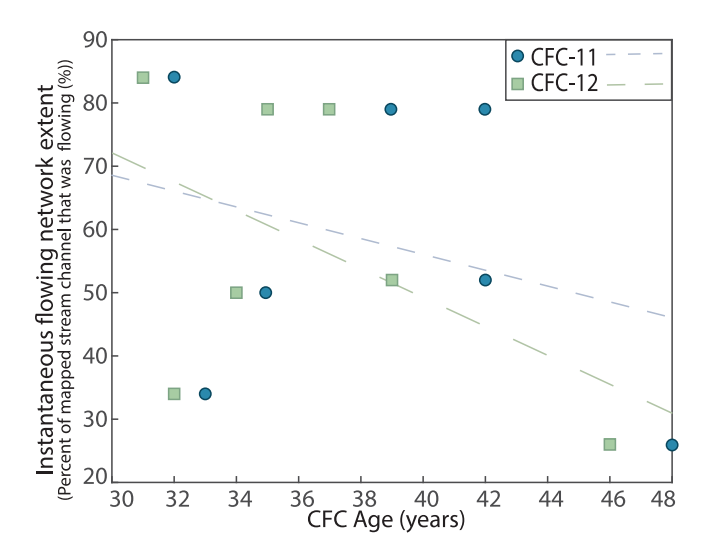


FIGURE 3 Instantaneous flowing network extent on August 5–6, 2019 is not correlated with CFC-11 (blue circles) or CFC-12 (green squares) spring ages. The poor correlation (CFC-11 $R^2=0.24$, CFC-12 $R^2=0.19$) suggests that groundwater age, as estimated at persistent springs, may be less important than shallow flowpaths or variations in losses further down the stream network in controlling flow permanence

was not significantly correlated with the instantaneous flowing network extent in early August (CFC-11: $R^2 = 0.24$, p value = 0.2688, and CFC-12: $R^2 = 0.19$, p value = 0.3280; Figure 3).

4.2 | Murphy Creek groundwater contributions and stream drying patterns

4.2.1 | Murphy Creek drying patterns

In Murphy Creek, flow was spatially continuous in June, but the stream gradually dried as the summer progressed. Peak flows occurred within the first 2 weeks of June at all four groundwater monitoring locations (Figure 5). Discharge was greatest at the outlet and usually decreased with increasing elevation at these monitoring locations (Table 2). At all sites, the lowest flows were measured in late August to early September. M1254 was the only monitoring location that did not dry, and it had a minimum discharge of <0.1 L/s. The uppermost reaches dried first and remained dry through the observation period (Figure 4). However, mid- and low-elevation sections also dried but at irregular intervals. Of the 25 network sensors, 22 were dry during peak contraction in early September for a seasonal (or minimum instantaneous) flowing network extent (Table 1) of only 12%. Discharge increased after a large storm in early September, and nine dry sites rewetted at that time, as determined from flow presence sensors.

4.2.2 | Murphy Creek specific conductivity

SC decreased with elevation for the four groundwater monitoring locations (Figure 5). At all groundwater monitoring locations, SC was

TABLE 2 Discharge, SC, and groundwater observations for the four groundwater monitoring locations

Sensor ID	Maximum Q (L/s)	Minimum SC > 0 (μS/cm)	Maximum SC (μS/cm)	Median GW flux (L/s)
M233	17	135	357	0.994
M759	11	131	219	0
M1254	8	108	263	0.251
M1799	4	67	134	0.107

FIGURE 4 Maps of Murphy Creek showing the seasonal flow permanence (a) and the first day that the stream was dry (b) for each of the 25 sensor locations. Seasonal flow permanence refers to the percentage of the observation period (June 1, 2019-Oct. 1, 2019) that surface water was flowing at each sensor location. The first day dry refers the day when the measurement indicated for the first time that the streambed was dry, but the location may have rewetted after this moment. Each metric is coloured using a blue-green-yellow colour scale where blue means that the location spent more time flowing (a) or dried late in the observation period (b)

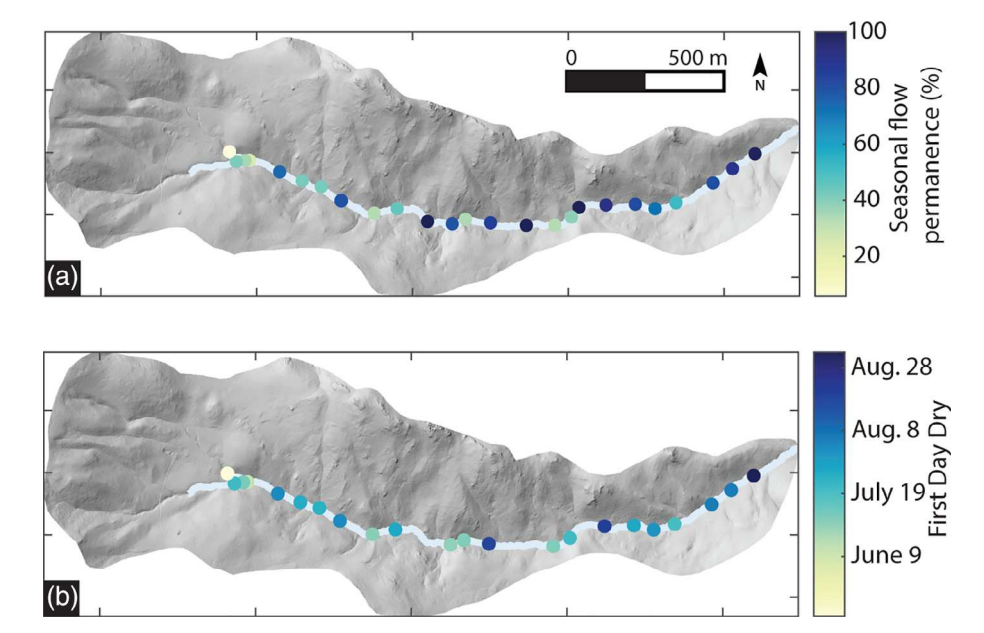
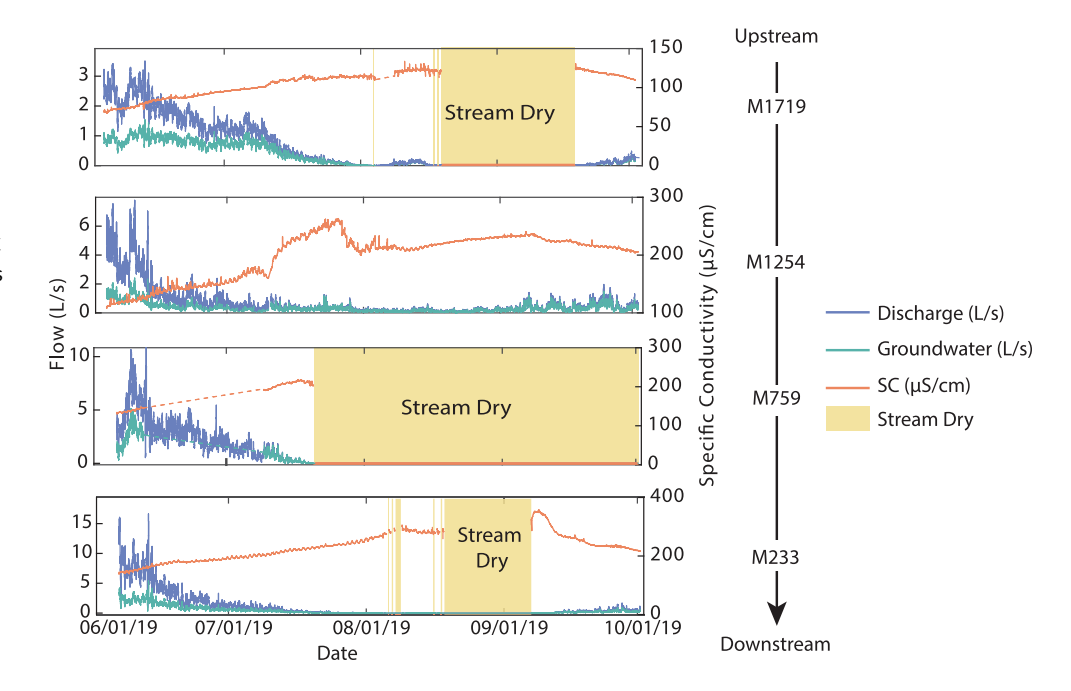


FIGURE 5 Discharge (L/s), groundwater (L/s), and SC (µS/cm) throughout the observation period at each of the four groundwater monitoring locations in Murphy Creek. Discharge and groundwater are plotted on the left y-axis while SC is plotted on the right y-axis. Plots are ordered from downstream (bottom) to upstream (top); the distance from the outlet weir is coded in the sensor name to the right of the plots using the notation MX where X refers to metres upstream from the outlet weir



lowest at the beginning of the observation period and increased as the summer progressed (Table 2). In all locations with flow at the end of the observation period on October 1, 2019 (including locations that sustained flow throughout the period and those that rewetted in September), SC began to drop by early September and

continued to decrease through the end of the observation period. Despite the consistency in seasonal patterns, SC at individual monitoring locations exhibited distinct diel cycling patterns (Figure 5) that varied with local evapotranspiration drivers as explored extensively in Warix (2020).

4.2.3 | Murphy Creek groundwater inputs

At all groundwater monitoring locations, the magnitude of the groundwater flux peaked early in the observation period, declined during the summer, and increased in early September after the onset of fall storms (Figures 5 and 6a). The magnitude of groundwater was more consistent throughout the observation period than discharge at the same location for each groundwater monitoring location (i.e., the standard deviation for groundwater was lower than that of discharge at the same location). Due to noise from complex diel fluctuations (Warix, 2020) and uncertainty in the flow measurements, a 2-week moving average was used to compare spatial and temporal patterns of the groundwater flux ($Q_{\rm GW}$). The only location that did not dry (M1254) had the lowest groundwater contribution flux at the

beginning of the observation period and the lowest variation in the groundwater flux as described by the standard deviation for the entire period (0.31 L/s). Groundwater magnitude at the three other sites peaked in June to early July, then decreased dramatically in mid-July before drying started.

Percent groundwater varied more among sites from mid-July through September than at the beginning of the observation period when groundwater was relatively low (Figures 6b). At the beginning of the observation period, when streamflow was high, percent groundwater increased over time at roughly similar rates across all sites. Percent groundwater was most similar at M233, M759, and M1799, the three groundwater monitoring locations that dried (Figure 6b). As flows decreased, the percent groundwater increased and typically peaked in late August to early September. The weekly

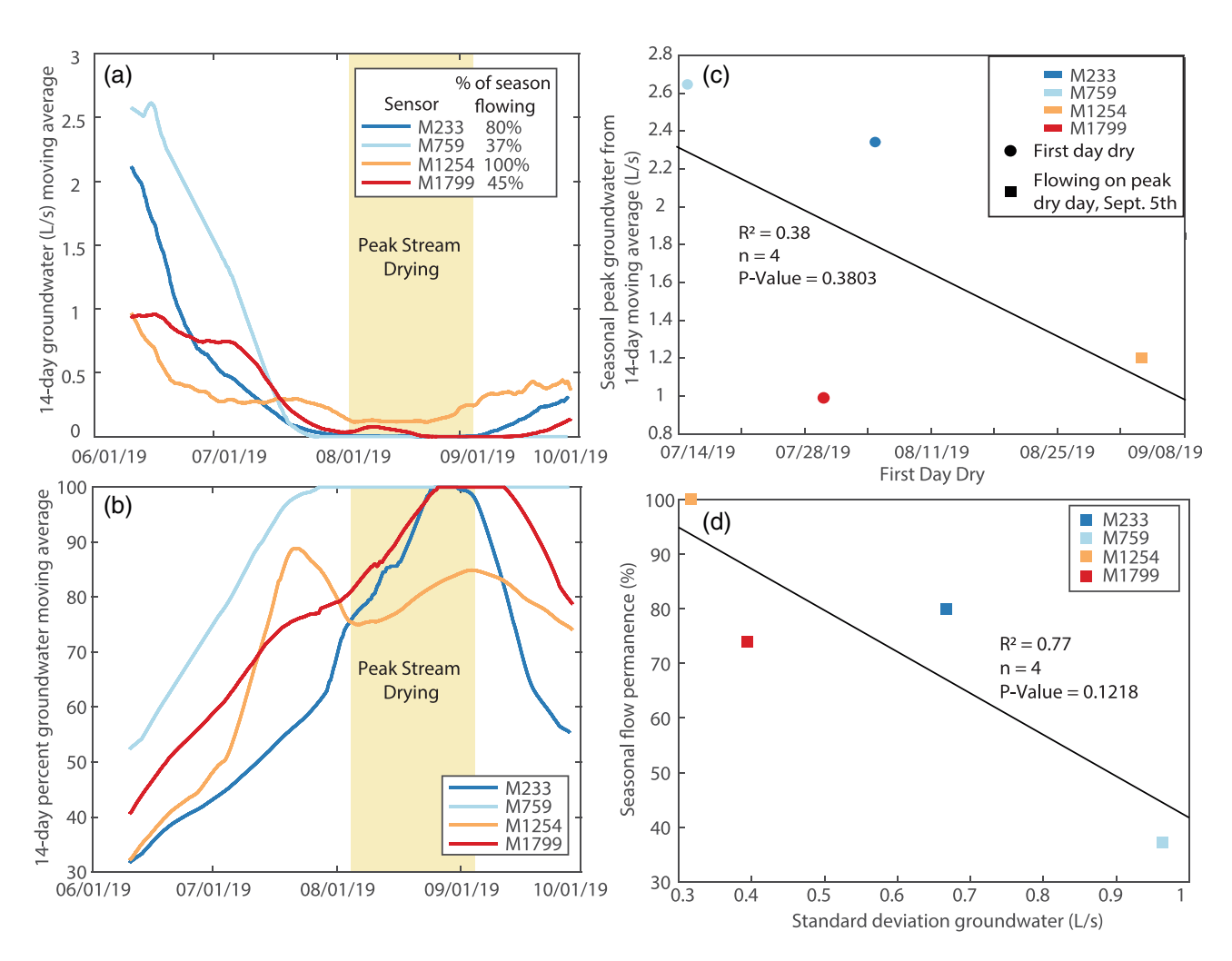


FIGURE 6 14-day moving average for groundwater flows, where groundwater is defined as an integrated signal from all deeper subsurface water entering the stream with high specific conductivity values (a), and 14-day moving average for percent groundwater (b) at the four groundwater monitoring locations in Murphy. A 14-day moving average was used to reduce noise at finer temporal scales because we are interested in patterns at the scale of the seasonal recession (see unfiltered data in Figure S1 in Data S1). Seasonal flow permanence (%, defined in Table 1) for a given location is summarised in the legend for each groundwater monitoring location in (a). The peak stream drying period (≤25% of sensors flowing) is shaded in yellow. Peak magnitude of groundwater calculated over a 14-day moving average dataset plotted against the first day dry (c), or in the case that the sensor did not dry (M1254), the day that most sensors were dry (September 5th, 2019). Sites with larger peaks in groundwater dried earlier and stayed dry. Seasonal flow permanence plotted against standard deviation of groundwater (d). At locations with more stable groundwater (i.e., those with a lower standard deviation or CV, as discussed in Section 4.2.3), the seasonal flow permanence is larger

rates of change in percent groundwater were less consistent among sites during the peak drying period. The magnitude of peak groundwater was negatively correlated with the first day of drying, but the relationship was not statistically significant ($R^2 = 0.38$, p value = 0.3803; Figure 6c). There was a non-significant negative relationship between the standard deviation of percent groundwater and seasonal flow permanence at the four locations in Murphy Creek ($R^2 = 0.77$, p value = 0.1218; Figure 6d), so that when percent groundwater was more stable, the stream was more likely to remain flowing. Seasonal flow permanence was also compared against the coefficient of variation (CV) for the groundwater flux and the same pattern was present, but weaker ($R^2 = 0.41$, p value = 0.412, not shown). While this relationship is based on only four observations, these findings suggest an interesting pattern that requires further inquiry.

4.2.4 | Discharge source and stream drying

We observed a strong negative relationship ($R^2=0.85$, p<0.0001) between the instantaneous flowing network extent (as measured by the presence absence sensors) and the average of the relative percent groundwater contributions (as determined for the four groundwater monitoring locations) during times of drying and rewetting in Murphy Creek (Figure 7). At the beginning of June, the stream was flowing continuously for at least 1994 metres above the outlet, and groundwater contributed less than 40% of total discharge (red points in

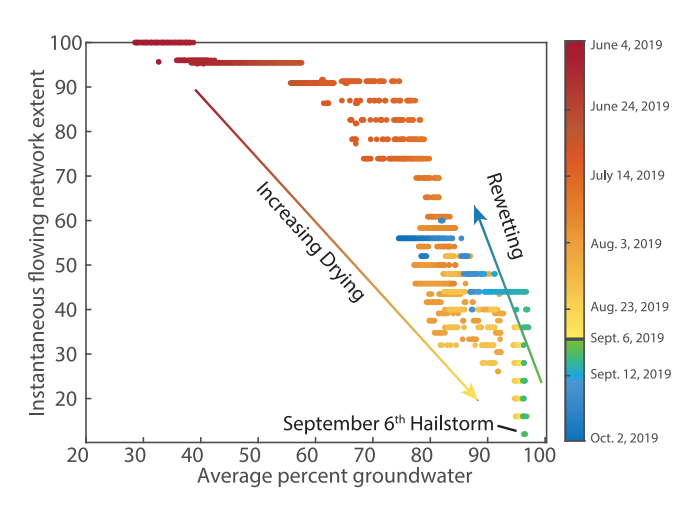


FIGURE 7 Average percent groundwater for the four groundwater monitoring locations at Murphy Creek plotted against the instantaneous flowing network extent, that is, the percent of sensors (n=25) that detected flow at the same timestep. Each point is coloured by time where warm colours (red to orange to yellow gradient) display the seasonal flow recession until peak stream drying and cool colours (green to blue gradient) display a rewetting period at the end of the observation period. Rewetting began after a heavy hailstorm on September 6th, 2019 that caused nine of 22 dry sensors to rapidly rewet. Trendlines showing increasing and decreasing groundwater patterns are displayed using the same colour gradient. If the stream was dry at a groundwater monitoring location, percent groundwater was assumed to be 100%

Figure 7) with flows instead mostly supported by (near-)surface runoff. The contribution of groundwater, as measured through the average percent groundwater, increased at each of the four sites as we observed drying progress from the 1st week in June. As additional sites continued to dry, the average percent groundwater at all monitoring locations increased at least through early July, except for M1254. Drying and percent groundwater continued to increase at most sites until September 6th when a large hailstorm caused nine of 22 dry sites to rewet rapidly and percent groundwater to decrease at all sites (Figure 7).

4.3 | Topographic metrics and stream drying

Elevation and slope were negatively correlated with seasonal flow permanence for each sensor location, whereas upstream contributing area and TWI were positively correlated with seasonal flow permanence (Figure 8 and Table 3). That is, stream locations that were dry the longest had a smaller TWI than locations where the flow persisted (Figure 8f). Steeper upstream locations with a lower TWI typically ceased flowing earlier (as indicated by the yellow and light green squares in Figure 8g), stayed dry longer, and did not rewet during September and October storms (as indicated by the dark blue and green circles in Figure 8g). Unsurprisingly, sites that were dry longer dried out earlier. However, the relationship between the initiation of drying and seasonal flow permanence was not a simple linear relationship. Instead, we observed a step change associated with those sites that rewetted following the September hailstorm (Figure 8g).

Curvature and down-valley subsurface area were poor predictors of seasonal flow permanence at each sensor location (Figure 8d,f). Although the down-valley subsurface area varied along the length of the stream (0 to 81 m², mean = 17 m²), it was not well correlated with other topographic attributes, such as channel slope ($R^2 = 0.002$, p value = 0.8344), upstream catchment area ($R^2 = 0.01$, p value = 0.8082), or TWI ($R^2 = .02$, p value = 0.8062) (not shown).

5 | DISCUSSION

5.1 | Groundwater residence time is not a reliable predictor of the instantaneous flowing network extent during a low-flow period

Because streamflow generation in perennial streams at larger scales is often driven by waters with deeper flowpaths and longer residence times (Frisbee et al., 2011), we hypothesised that groundwater residence times in headwater streams that are seasonally sustained by groundwater contributions would be reliably predict the extent of surface flows within that headwater stream network. However, this hypothesis was not supported in sub-catchments within the RC CZO. Although groundwater residence times vary by two or more orders of magnitude globally (Bethke & Johnson, 2008), we observed a relatively small range of residence times (\sim 16 years, or a \sim 50% increase in age

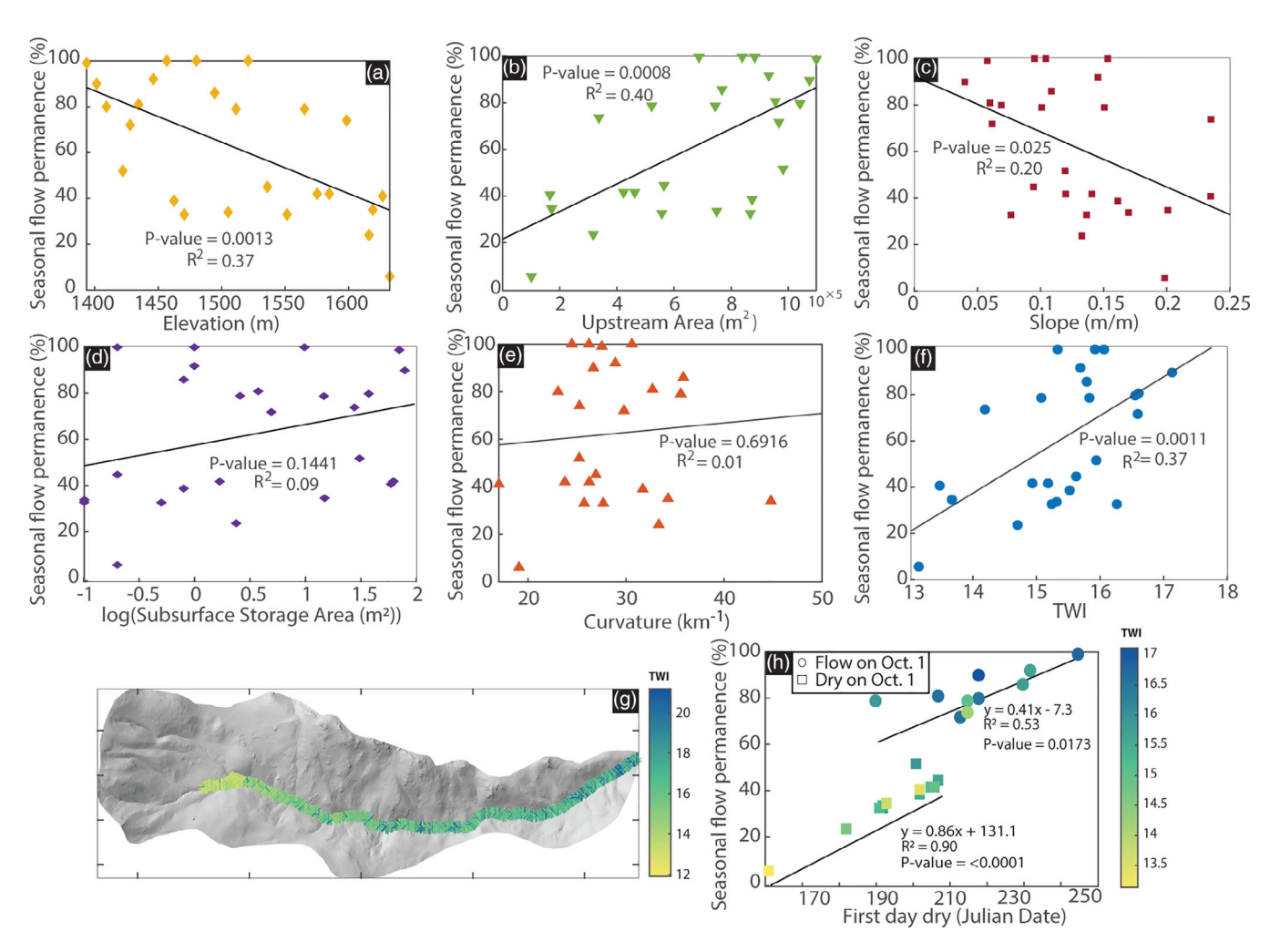


FIGURE 8 Regression between the seasonal flow permanence at each of the 25 Murphy Creek sensors (21 presence/absence and 4 groundwater sensors) and topographic metrics, including elevation (a), upstream contributing area (b), slope (c), the log-transformed subsurface area along the stream corridor (d), curvature (e), and the topographic wetness index (f). In panel (d), very small (<1 m²) subsurface areas exist where the valley is deeply incised; log-transformed storage area is plotted to account for this skewed distribution. Panel (g) presents a DEM of Murphy Creek with the creek coloured by TWI and the creek width exaggerated. Panel (h) highlights the relationship between TWI and drying/rewetting patterns. In this panel, symbol colour represents TWI and symbol shape indicates whether the sensor had rewetted by October 1, 2019 (the three sensors that had continuous flow throughout the observation period are excluded from this panel). Seasonal flow permanence varies with first day dry: those locations that did not rewet also dried earlier in the observation period and typically have lower TWI values. In contrast, locations with higher TWI typically dried later in the observation period and rewetted after the onset of fall storms. Upstream catchment area serves as the best individual predictor of seasonal flow permanence

from the youngest to oldest waters). Our observations are consistent with evidence that deep groundwater flow is not the main driver of variability in specific discharge in headwater catchments in Switzerland (Floriancic et al., 2019). Even though groundwater emerged at each spring we sampled, we observed that drying sometimes occurred within tens of metres of the spring outlet. It is possible that local subsurface controls that lead to groundwater emerging at a spring may impede downstream groundwater contributions that might otherwise sustain surface flows, or that streambed properties are more important than deep groundwater flowpaths that feed the springs in controlling the presence of water in-stream networks below springs.

Spring groundwater residence times (CFC-11 = 32-48 years, CFC-12 = 31-46 years) were somewhat longer than residence times from similar headwater catchments with frequent and extensive

stream drying. For example, a wider range of ages, including shorter groundwater residence times have been observed in high-elevation springs in the headwater Sagehen Basin in Truckee, CA where groundwater residence times in $a\sim27~{\rm km^2}$ basin ranged from 10 to 36 years (Rademacher et al., 2001). In the West Fork catchment in Utah ($\sim181~{\rm km^2}$), residence times in high-elevation springs ranged from 3 to 33 years (Georgek et al., 2018). We hypothesise that the relatively older groundwater at Reynolds Creek (as compared to the other headwater catchments summarised here) may indicate that Reynolds' headwater streams are sourced by a combination of both local and deeper or regional groundwater flow. Alternatively, the longer residence times may suggest slower local transmissivity, although this is inconsistent with observed patterns of diel cycling of water levels during low-flow periods in Murphy Creek (Kirchner et al., 2020;

TABLE 3 Topographic and seasonal flow permanence at each sensor in Murphy, with sensor and location information detailed in Sections 3.2–3.4

Sensor ID	Seasonal flow permanence (%) ^a	Slope (m/m)	Upstream contributing area (km²)	Curvature (km ⁻¹)	TWI (m/m/ln[m ²])	Subsurface storage area (m²)
M91	99.1	0.057	1.10	27.53	16.8	72.5
M153	89.8	0.040	1.07	26.66	17.1	81.4
M233	80.1	0.069	1.04	23.06	16.5	38.3
M380	51.5	0.119	0.98	25.22	15.9	31.6
M454	71.8	0.061	0.97	29.79	16.6	5
M523	81.4	0.060	0.95	32.70	16.6	3.8
M624	92.1	0.145	0.93	28.90	15.7	0
M716	100	0.095	0.88	26.22	16.0	0.2
M759	39.2	0.161	0.87	31.70	15.5	0.8
M823	33.2 (10.0)	0.076	0.87	25.73	16.2	0.1
M918	100	0.104	0.84	24.47	15.9	10
M1036	86.3	0.108	0.77	35.85	15.8	0.8
M1121	34.3 (11.1)	0.170	0.75	44.79	15.3	0.1
M1166	78.7 (54.6)	0.101	0.74	35.61	15.8	2.6
M1254	100	0.153	0.69	30.59	15.3	0
M1377	45.4	0.094	0.56	26.93	15.6	0.2
M1452	32.9	0.136	0.56	27.67	15.2	0.5
M1572	79.1	0.150	0.52	35.57	15.1	15
M1653	42.5 (31.2)	0.120	0.46	23.76	15.2	64.2
M1719	41.8	0.140	0.42	26.25	14.9	1.7
M1799	73.6 (70.2)	0.235	0.34	25.25	14.2	28.4
M1909	24.1	0.132	0.32	33.34	14.7	2.4
M1951	35.2	0.201	0.17	34.29	13.7	15.3
M1984	40.6	0.235	0.17	17.02	13.5	61
M1993	5.9	0.198	0.10	19.08	13.1	0.2

Note: Briefly, sensor ID Mxxx is the distance in metres above the Murphy outlet weir, seasonal flow permanence is calculated from 25 presence/absence sensors, and the remaining topographic and subsurface storage metrics are determined from a LiDAR-derived DEM.

Warix, 2020). Finally, surface water integrates multiple groundwater sources, which may limit the use of springs as a proxy for stream groundwater inputs if their flowpaths differ and diffuse inputs exceed spring contributions. It would be worthwhile to expand the spatial extent of this analysis to test whether residence time is a stronger predictor over a wider range of potential groundwater residence times, climatic conditions, and stream permanence.

5.2 | Groundwater inputs and stream drying in Murphy Creek

5.2.1 | Stable groundwater flux may lead to persistent stream flow

Although groundwater age was not a good predictor of the instantaneous network extent, we still hypothesised that more stable

groundwater inputs would ensure seasonal flow permanence at any given point along the stream network. Our end-member observations support this hypothesis (Figure 6), but the small number of observations and uncertainty in our measurements limit our ability to draw a strong conclusion from our data. While the site with the smallest variation in the relative groundwater contribution did not dry, another site with low variation in groundwater inputs was dry the longest of the four (Figure 6d). Nonetheless, the groundwater variation-drying trend is intriguing, and future studies should expand the sample size to more rigorously test this hypothesis. We also recommend that future efforts consider the inherently large uncertainty of barometric corrections of unvented pressure transducers at low flows: small differences in relatively large pressure measurements will inevitably lead to uncertain low-flow estimates and this potentially limits the inferences from such measurements. Stable groundwater inputs are important because stream drying occurs when runoff and groundwater combined can no longer sustain surface water presence. In the RC

^aFor the six sensors that were missing observations due to sensor failure, we include a second seasonal flow permanence estimate in parentheses that assumes that the stream is dry, even though adjacent monitoring locations are flowing during the entire gap in each case. A sensitivity analysis reveals that our conclusions in Figure 8 are not substantially altered by the uncertainty between these two values for these sensors.

CZO region, like many arid and semi-arid areas, precipitation inputs are highly seasonal, so it would make sense that streamflow is able to persist during the dry summer only in areas with steady groundwater inputs. This is consistent with the substantial network drying that began after the near-surface flow component to discharge declined (Figure 6a,b) and observations elsewhere (e.g., Kirchner et al., 2020) that groundwater and surface water fluctuations are often tightly coupled.

However, it is also possible that the relationship between groundwater stability and drying is not consistent over space, perhaps explaining the variability that we observed in Figure 6d. For example, it appears that the local hydrologic characteristics at M1254 are more conducive to groundwater flow than at the other Murphy monitoring locations, and it would be useful to assess whether subsurface structures around this location are different (e.g., shift in weathering depth, fracture density, or hydraulic conductivity) because subsurface characteristics controls groundwater flowpaths (Mwakalila et al., 2002; Payn et al., 2012; Segura et al., 2019). To maintain surface flows from groundwater inputs along the length of a stream network, groundwater discharge must overcome losses from evapotranspiration and to the streambed (Payn et al., 2012; Winter, 2007) either by continuous additions along the length of the stream or sufficiently large contributions at discrete locations. Our observations are consistent with this concept as areas without stable groundwater flow dried quickly (Figure 6a,c). While not tested here, others, such as Zimmer and McGlynn (2017b) and Dohman (2018), have highlighted the potential importance of multiple subsurface flowpaths contributing to flow during low-flow periods. Here, we show that stream drying is more likely where these groundwater inputs are unstable and suggest that the primary controls on groundwater are also important for streamflow permanence studies.

5.2.2 | Stream drying more likely when percent groundwater is high

We also asked how groundwater inputs and stream drying were related over time and hypothesised that at local scales, larger groundwater inputs would ensure stream flow permanence. Similar to Zimmer and McGlynn (2017b), we found weak evidence that streamflow persists when groundwater inputs are high. However, in contrast to their study, we observed the smallest instantaneous flowing network extent when percent groundwater peaked (Figure 7). That is, although local streamflow can persist at locations where groundwater inputs are stable, the timing of network-scale stream drying coincides with a high percent of the stream sourced by groundwater. This makes sense in intermittent systems because percent groundwater increases when both surface inputs and total discharge in the system are low.

Although groundwater can sustain streams during low-flow periods between precipitation events (Freeze, 1974; Godsey et al., 2013; Segura et al., 2019), few studies have quantified the fraction of groundwater and flow persistence during times of stream network contraction

and expansion (Queener, 2015). Our study reveals a threshold-based relationship between stream drying and the primary source of stream flow (i.e., groundwater or runoff) within Murphy Creek. The instantaneous flowing network extent was insensitive to average percent groundwater until a threshold of ~40% groundwater, above which we observed a negative correlation between instantaneous flowing network extent and average percent groundwater (Figure 7). We acknowledge that if the groundwater SC signature exhibits a seasonal trend, then the observed threshold could shift or appear as a more abrupt step change. Because we did not have access to a well to determine the seasonal groundwater SC signature, we assumed it was seasonally constant (following Miller et al., 2014; Saraiva Okello et al., 2018). If groundwater contributions had already reached 100% by mid-July and groundwater SC were simply increasing after this point, our results would be qualitatively similar, but shifted in time with a more abrupt increase in the percent groundwater contributions. Furthermore, we note that the relationship we observed in Figure 7 likely does not capture the full range of drying patterns because the stream had already expanded and contracted above our uppermost sensors prior to the observation period; seasonal snowpack had mostly melted before we instrumented the catchment in June. For example, compared to our mapped network. MacNeille et al. (in review) observed that the flowing length in Murphy Creek was ~800 m longer in April 2016, 1 year after the Soda Fire. Nonetheless, we expect that an expanded observation period would only scale the x-axis in Figure 7, shifting the threshold at which groundwater and seasonal flow permanence were strongly negatively correlated.

During our field visits, we observed moist soils in the hillslope or stream corridor in June and July that dried by August, and could serve as potential near-surface flow sources, broadly corroborating the inferred contributions. Hillslope soils in Reynolds Creek are known to rapidly dry during summer drought periods (Seyfried et al., 2018), so it would be worth verifying these inferences with additional highfrequency soil moisture measurements, but that was outside the scope of this project. After the early September hailstorm when discharge increased, the slope of the stream network-groundwater relationship (Figure 7) was the same as prior to rewetting, showing that the relationship between groundwater and the flowing network extent is the same during drying and rewetting periods, in contrast to observed hysteresis in wetting and drying in more humid headwater streams (Jensen et al., 2019). The rapid rewetting event also demonstrated that precipitation can quickly reconnect subsurface and surface flows if: (1) precipitation inputs are greater than the subsurface discharge rate from previously disconnected hillslope storage to the stream, or (2) stream corridor transmissivity and hydraulic conductivity is small enough for subsurface flow to accumulate and contribute to surface flows.

5.3 | Topographic metrics as proxies for stream drying potential

We hypothesised that topographic metrics would be good predictors of flow permanence, and indeed we found moderately strong relationships between seasonal flow permanence and slope, upstream catchment area, elevation, and TWI (Figure 8). We found that stream drying is probable where the upstream contributing area is small and slope is high: stream segments with low TWI were dry for a greater period of time (Figure 8b,c,f), consistent with the work of Prancevic and Kirchner (2019). However, we did not find a correlation between stream permanence and local curvature (Figure 8e), in contrast to the work of Whiting and Godsey (2016) and Prancevic and Kirchner (2019). The poor relationship between seasonal flow permanence and curvature at Murphy Creek may be because (1) the subsurface structure controlling groundwater is not always well reflected in curvature, or (2) the 2015 Soda Fire altered soil development and/or patterns of evapotranspiration losses despite other work showing postfire recovery within ~2 years (Vega et al., 2020). Topography often affects groundwater flow by driving depth to bedrock and flow gradients (Mueller et al., 2013; Mwakalila et al., 2002; Price, 2011; Segura et al., 2019) and modulating flow partitioning between the subsurface and surface (Prancevic & Kirchner, 2019), particularly when groundwater is dominant during low-flow periods (Segura et al., 2019). Indeed, we also showed that seasonal flow permanence is correlated with percent groundwater (Figures 6d and 7).

Although flow permanence was correlated with topographic metrics, they did not fully predict drying patterns, and thus it is currently unclear whether (1) topography is directly correlated with hydraulic head, a key driver of groundwater fluxes, and thus the probability of streams flowing throughout the season, or (2) if topography impacts subsurface properties such as hydraulic conductivity that dictate the ease with which water can pass through the subsurface, therefore controlling groundwater and subsequently stream drying. Topography may potentially influence hydraulic conductivity in two ways: first. through a relationship between topography and surface stress fields that may affect fracture density and thus conductivity (Clair et al., 2015), and second, through the relationship between topography and depth to weathered bedrock coupled with the typical exponential decay in hydraulic conductivity with depth. Current stream drying prediction models have assumed a constant hydraulic conductivity throughout the length of the stream network and assessed down-valley subsurface capacity by assuming that the slope of the valley bottom is a good approximation of the hydraulic gradient (Ward et al., 2018). Down-valley subsurface capacity may vary with valley width, colluvium depth, slope, and heterogeneity in hydraulic conductivity (Fleckenstein et al., 2006; Godsey & Kirchner, 2014; Ward et al., 2018). If subsurface flows are an important driver of drying and hydraulic conductivity is assumed to be constant, then down-valley capacity (represented by slope and area, or the valley width and colluvium depth) should vary with seasonal flow permanence. However, we estimated the down-valley subsurface area based on the DEM assuming an underlying V-shaped valley with a distinct valley bottom fill detectable by a slope break within the valley corridor (see Section 3.4 for details) and found that it is poorly correlated with seasonal flow permanence at any given location (Figure 8d). This finding leads us to conclude that either the assumptions underlying our estimate of the down-valley area were incorrect or that variations in hydraulic conductivity may strongly influence stream permanence. The latter inference would be consistent with low-flow modelling by Fleckenstein et al. (2006) and observations by Dohman (2018), but such measurements were beyond the scope of our study. Future stream drying studies and models would benefit from intensive geophysical characterisation of the down-valley capacity as well as hydraulic conductivity measurements, despite the time and expenses involved.

6 | CONCLUSION

Groundwater residence times, spatiotemporally dense assessments of groundwater contributions to the stream and stream drying patterns, as well as topographic metrics were used to establish the relationships between stream drying and groundwater. Groundwater residence times were poorly correlated with seasonal flow permanence and even the presence of old groundwater (>20 years) in the subsurface does not guarantee surface flow throughout the stream network. Over the observation period, stream drying across a stream network is most probable when runoff from near-surface flow pathways is minimal and streamflow is dominated by groundwater. However, at locations where groundwater inputs are seasonally stable, surface flows tend to persist, even as flows decrease. Finally, we show that seasonal flow permanence is correlated with topographic metrics. such as the upstream contributing area, elevation, slope, and TWI. Despite the observed connections between stream drying, groundwater inputs, and topographic metrics, over half of the observed variation in seasonal flow permanence remains unexplained. Thus frustratingly, predicting the instantaneous flowing network extent remains elusive. We suggest that geophysical characterisation of down-valley capacity and hydraulic conductivity measurements are important to determine the subsurface controls on the flowing stream network extent to better understand heterogeneity in-stream drying.

ACKNOWLEDGEMENTS

We would like to thank the USDA-Agricultural Research Service, particularly Zane Cram, Barry Caldwell, Mark Seyfried, and Alex Boehm. In addition, we would like to thank NSF [#1653998 & RC CZO Coop Agreement EAR 1331872], Exxon Mobil, the Idaho State University Geslin Fund, and the Geological Society of America for project funding. Thank you to Jeff Prancevic for assistance with TopoToolbox. Finally, we would like to thank Inbar Milstein, Chris Santore, Madison Skinner, Madison Thibado, Drew Wolford, and Logan Mahoney for field assistance.

DATA AVAILABILITY STATEMENT

The data that support the findings of this study are available at 10.18122/reynoldscreek/22/boisestate.

ORCID

Sara R. Warix https://orcid.org/0000-0003-2509-6849
Sarah E. Godsey https://orcid.org/0000-0001-6529-7886

Kathleen A. Lohse https://orcid.org/0000-0003-1779-6773
Rebecca L. Hale https://orcid.org/0000-0002-3552-3691

REFERENCES

- Bethke, C. M., & Johnson, T. M. (2008). Groundwater age and groundwater age dating. *Annual Review of Earth and Planetary Sciences*, *36*(1), 121–152. https://doi.org/10.1146/annurev.earth.36.031207.124210
- Beven, K. J., & Kirkby, M. J. (1979). A physically based, variable contributing area model of basin hydrology. *Hydrological Sciences Bulletin*, 24(1), 43–69. https://doi.org/10.1080/02626667909491834
- Burns, D. A., Plummer, L. N., McDonnell, J. J., Busenberg, E., Casile, G. C., Kendall, C., Hooper, R. P., Freer, J. E., Peters, N. E., Beven, K., & Peter, S. (2003). The geochemical evolution of riparian groundwater in a forested piedmont catchment. *Groundwater*, 41(7), 913–925. https://doi.org/10. 1111/j.1745-6584.2003.tb02434.x
- Busch, M. H., Costigan, K. H., Fritz, K. M., Datry, T., Krabbenhoft, C. A., Hammond, J. C., Zimmer, M., Olden, J. D., Burrows, R., Dodds, W. K., Boersma, K., Shanafield, M., Kampf, S. K., Mims, M. C., Bogan, M., Ward, A. S., Roch, M. P., Godsey, S., Allen, G., ... Allen, D. C. (2020). What's in a name? Patterns, trends, and suggestions for defining nonperennial rivers and streams. Water, 12, 1–19.
- Carey, S. K., Boucher, J. L., & Duarte, C. M. (2013). Inferring groundwater contributions and pathways to streamflow during snowmelt over multiple years in a discontinuous permafrost subarctic environment (Yukon, Canada). *Hydrogeology Journal*, 21(1), 67–77. https://doi.org/ 10.1007/s10040-012-0920-9
- Carroll, R. W. H., Bearup, L. A., Brown, W., Dong, W., Bill, M., & Willlams, K. H. (2018). Factors controlling seasonal groundwater and solute flux from snow-dominated basins. *Hydrological Processes*, 32 (14), 2187–2202. https://doi.org/10.1002/hyp.13151
- Center, U. A. N. W. R. CR. (2020). Precipitation-Reynolds Creek experimental watershed-(1962-ongoing). HydroShare. Retrieved from https://www.hydroshare.org/resource/701e2a6bdad942aca5b7014bb574dfe3/
- Chapin, T. P., Todd, A. S., & Zeigler, M. P. (2014). Robust, low-cost data loggers for stream temperature, flow intermittency, and relative conductivity monitoring. *Water Resources Research*, 50(8), 6542–6548. https://doi.org/10.1002/2013WR015158
- Clair, J. S., Moon, S., Holbrook, W. S., Perron, J. T., Riebe, C. S., Martel, S. J., Carr, B., Harman, C., Singha, K., & De Richter, D. B. (2015). Geophysical imaging reveals topographic stress control of bedrock weathering. *Science*, 350(6260), 534–538. https://doi.org/10. 1126/science.aab2210
- Costigan, K. H., Jaeger, K. L., Goss, C. W., Fritz, K. M., & Goebel, P. C. (2016). Understanding controls on flow permanence in intermittent rivers to aid ecological research: Integrating meteorology, geology and land cover. *Ecohydrology*, 9(7), 1141–1153. https://doi.org/10.1002/eco.1712
- Dohman, J. (2018). Three-dimensional subsurface controls on stream intermittency in a semi-arid landscape. Idaho State University.
- Earman, S., & Dettinger, M. (2011). Potential impacts of climate change on groundwater resources-A global review. *Journal of Water and Climate Change*, 2(4), 213–229. https://doi.org/10.2166/wcc.2011.034
- Eng, K., Wolock, D. M., & Dettinger, M. D. (2015). Sensitivity of intermittent streams to climate variations in the USA. River Research and Applications, 32, 885–895. https://doi.org/10.1002/rra
- Erman, N. A., & Erman, D. C. (1995). Spring permanence, Trichoptera species richness, and the role of drought. *Journal of the Kansas Entomological Society*, 68(2), 50–64.
- Fleckenstein, J. H., Niswonger, R. G., & Fogg, G. E. (2006). River-aquifer interactions, geologic heterogeneity, and low-flow management. *Ground Water*, 44, 837–852. https://doi.org/10.1111/j.1745-6584.2006.00190.x
- Floriancic, M. G., Fischer, B. M. C., Molnar, P., Kirchner, J. W., & van Meerveld, I. H. J. (2019). Spatial variability in specific discharge and streamwater chemistry during low flows: Results from snapshot

- sampling campaigns in eleven Swiss catchments. *Hydrological Processes*, 33(22), 2847–2866. https://doi.org/10.1002/hyp.13532
- Freeze, R. A. (1974). Streamflow generation. *Reviews of Geophysics*, 12(4), 627–647. https://doi.org/10.1029/RG012i004p00627
- Frisbee, M. D., Phillips, F. M., Campbell, A. R., Liu, F., & Sanchez, S. A. (2011). Streamflow generation in a large, alpine watershed in the southern Rocky Mountains of Colorado: Is streamflow generation simply the aggregation of hillslope runoff responses? Water Resources Research, 47(6), 1–18. https://doi.org/10.1029/2010WR009391
- Frisbee, M. D., Tolley, D. G., & Wlilson, J. L. (2017). Field estimates of groundwater circulation depths in two mountainous watersheds in the western U.S. and the effect of deep circulation on solute concentrations in streamflow. *Water Resources Research*, 53, 2693–2715. https://doi.org/10.1111/j.1752-1688.1969.tb04897.x
- Georgek, J. L., Kip Solomon, D., Heilweil, V. M., & Miller, M. P. (2018). Using tracer-derived groundwater transit times to assess storage within a high-elevation watershed of the upper Colorado River basin, USA. Hydrogeology Journal, 26, 467–480. https://doi.org/10.1007/ s10040-017-1655-4
- Ghosh, D. K., Wang, D., & Zhu, T. (2016). On the transition of base flow recession from early stage to late stage. *Advances in Water Resources*, 88, 8–13. https://doi.org/10.1016/j.advwatres.2015.11.015
- Godsey, S. E., & Kirchner, J. W. (2014). Dynamic, discontinuous stream networks: Hydrologically driven variations in active drainage density, flowing channels and stream order. *Hydrological Processes*, 28(23), 5791–5803. https://doi.org/10.1002/hyp.10310
- Godsey, S. E., Kirchner, J. W., & Tague, C. L. (2013). Effects of changes in winter snowpacks on summer low flows: Case studies in the Sierra Nevada, California, USA. *Hydrological Processes*, 28, 5048–5064. https://doi.org/10.1002/hyp.9943
- Gutiérrez-Jurado, K. Y., Partington, D., Batelaan, O., Cook, P., & Shanafield, M. (2019). What triggers streamflow for intermittent rivers and ephemeral streams in low-gradient catchments in mediterranean climates. Water Resources Research, 55(11), 9926–9946. https://doi.org/10.1029/2019WR025041
- Hale, C. V., & McDonnell, J. J. (2016). Effect of bedrock permeability on stream base flow mean transit time scaling relations: 1. A multiscale catchment intercomparison. Water Resources Research, 55(2), 1358– 1374. https://doi.org/10.1111/j.1752-1688.1969.tb04897.x
- Hall, F. R. (1968). Base-flow recessions—A review. Water Resources Research, 4(5), 973–983. https://doi.org/10.1029/WR004i005p00973
- Hooper, R. P., & Shoemaker, C. A. (1986). A comparison of chemical and isotopic hydrograph separation. Water Resources Research, 22(10), 1444–1454. https://doi.org/10.1029/WR022i010p01444
- Ilangakoon, N., Glenn, N. F., Spaete, L. P., Dashti, H., & Li, A. (2016). 2014 lidar-derived 1m digital elevation model data set for Reynolds Creek Experimental Watershed, Southwestern Idaho. http://doi.org/10. 18122/B26C7X
- Jaeger, K. L., Sando, R., McShane, R. R., Dunham, J. B., Hockman-Wert, D. P., Kaiser, K. E., Hafen, K., Risley, J. C., & Blasch, K. W. (2019). Probability of streamflow permanence model (PROSPER): A spatially continuous model of annual streamflow permanence throughout the Pacific northwest. *Journal of Hydrology X*, 2, 100005. https://doi.org/10.1016/J.HYDROA.2018.100005
- Jensen, C. K., McGuire, K. J., McLaughlin, D. L., & Scott, D. T. (2019). Quantifying spatiotemporal variation in headwater stream length using flow intermittency sensors. *Environmental Monitoring and Assessment*, 191(4), 226. https://doi.org/10.1007/s10661-019-7373-8
- Kirchner, J., Godsey, S., Osterhuber, R., McConnell, J., & Penna, D. (2020). The pulse of a montane ecosystem: Coupled daily cycles in solar flux, snowmelt, transpiration, groundwater, and streamflow at Sagehen and Independence creeks, Sierra Nevada, USA. Hydrology and Earth System Sciences Discussions. pp. 1–46. https://doi.org/10.5194/hess-2020-77

- Kirchner, J. W. (2009). Catchments as simple dynamical systems: Catchment characterization, rainfall-runoff modeling, and doing hydrology backward. Water Resources Research, 45(2), 1–34. https://doi.org/10.1029/2008WR006912
- Klaus, J., & McDonnell, J. J. (2013). Hydrograph separation using stable isotopes: Review and evaluation. *Journal of Hydrology*, 505, 47–64. https://doi.org/10.1016/j.jhydrol.2013.09.006
- Klos, Z. P., Link, T. E., & Abatzoglou, J. T. (2014). Extent of the rain-snow transition zone in the western U.S. under historic and projected climate. *Geophysical Research Letters*, 41, 6413–6419. https://doi.org/ 10.1002/2014GL061184
- Kolbe, T., Marçais, J., Thomas, Z., Abbott, B. W., de Dreuzy, J. R., Rousseau-Gueutin, P., Aquilina, L., Labasque, T., & Pinay, G. (2016). Coupling 3D groundwater modeling with CFC-based age dating to classify local groundwater circulation in an unconfined crystalline aquifer. *Journal of Hydrology*, 543, 31–46. https://doi.org/10.1016/j. jhydrol.2016.05.020
- Kormos, P. R., Marks, D., Seyfried, M., Havens, S., Hendrick, A., Lohse, K. A., Masarik, M., & Flores, A. N. (2016). 31 years of spatially distributed air temperature, humidity, precipitation amount and precipitation phase from a mountain catchment in the rain-snow transition zone. https://doi.org/10.18122/B2B59V
- Laudon, H., Seibert, J., Köhler, S., & Bishop, K. (2004). Hydrological flow paths during snowmelt: Congruence between hydrometric measurements and oxygen 18 in meltwater, soil water, and runoff. Water Resources Research, 40(3), 1–9. https://doi.org/10.1029/2003WR002455
- Levick, L. R., Goodrich, D. C., Hernandez, M., Fonseca, J., Semmens, D. J., Stromberg, J., Tluczek, M., Leidy, R. A., Scianni, M., & Guertin, D. P. (2008). The ecological and hydrological significance of ephemeral and intermittent Streams in the arid and semi-arid American Southwest. Retrieved from www.epa.gov
- Liu, F., Hunsaker, C., & Bales, R. C. (2013). Controls of streamflow generation in small catchments across the snow-rain transition in the southern Sierra Nevada, California. *Hydrological Processes*, 27(14), 1959–1972. https://doi.org/10.1002/hyp.9304
- Lovill, S. M., Hahm, W. J., & Dietrich, W. E. (2018). Drainage from the critical zone: Lithologic controls on the persistence and spatial extent of wetted channels during the summer dry season. Water Resources Research, 54 (8), 5702–5726. https://doi.org/10.1029/2017WR021903
- Lundquist, J. D., Dettinger, M. D., Stewart, I. T., & Cayan, D. R. (2009). Variability and trends in spring runoff in the Western United States. Climate Warming in western North America. Evidence and environmental effects. (January 2014). pp. 1–35.
- MacNeille, R. B., Lohse, K. A., Godsey, S. E., & Perdrial, J. N. (2020). Influence of drying and wildfire on longitudinal chemistry patterns and processes of intermittent streams. Frontiers in Water, 2, 42. https://doi.org/10.3389/frwa.2020.563841
- Manning, A. H., Clark, J. F., Diaz, S. H., Rademacher, L. K., Earman, S., & Niel, P. L. (2012). Evolution of groundwater age in a mountain water-shed over a period of thirteen years. *Journal of Hydrology*, 460–461, 13–28. https://doi.org/10.1016/j.jhydrol.2012.06.030
- Matsubayashi, U., Velasquez, G. T., & Takagi, F. (1993). Hydrograph separation and flow analysis by specific electrical conductance of water. *Journal of Hydrology*, 152(1-4), 179-199. https://doi.org/10.1016/0022-1694(93)90145-Y
- Maurya, A. S., Shah, M., Deshpande, R. D., Bhardwaj, R. M., Prasad, A., & Gupta, S. K. (2011). Hydrograph separation and precipitation source identification using stable water isotopes and conductivity: River ganga at Himalayan foothills. *Hydrological Processes*, 25(10), 1521–1530. https://doi.org/10.1002/hyp.7912
- Maxwell, R. M., Condon, L. E., Kollet, S. J., Maher, K., Haggerty, R., & Forrester, M. M. (2015). The imprint of climate and geology on the residence times of groundwater. *Geophysical Research Letters*, 43, 701–708. https://doi.org/10.1002/2015GL066916

- McDonnell, J. J., Sivapalan, M., Vaché, K., Dunn, S., Grant, G., Haggerty, R., Hinz, C., Hooper, R., Kirchner, J., Roderick, M. L., Selker, J., & Weiler, M. (2007). Moving beyond heterogeneity and process complexity: A new vision for watershed hydrology. Water Resources Research, 43(7), W07301. https://doi.org/10.1029/2006WR005467
- Miller, M. P., Susong, D. D., Shope, C. L., Heilweil, V. M., & Stolp, B. J. (2014). Continuous estimation of baseflow in snowmelt-dominated streams and rivers in the upper Colorado River basin: A chemical hydrograph separation approach. Water Resources Research, 50(8), 6986–6999. https://doi.org/10.1002/2013WR014939
- Moore, R. D. D. (2003). Introduction to salt dilution gauging for streamflow measurement: Part 1. Streamline, Watershed Management Bulletin, 7(4), 20–23.
- Mote, P. W., Li, S., Lettenmaier, D. P., Xiao, M., & Engel, R. (2018). Dramatic declines in snowpack in the western US. npj Climate and Atmospheric Science, 1(1), 2. https://doi.org/10.1038/s41612-018-0012-1
- Mueller, M. H., Weingartner, R., & Alewell, C. (2013). Importance of vegetation, topography and flow paths for water transit times of base flow in alpine headwater catchments. *Hydrology and Earth System Sciences*, 17(4), 1661–1679. https://doi.org/10.5194/hess-17-1661-2013
- Mwakalila, S., Feyen, J., & Wyseure, G. (2002). The influence of physical catchment properties on baseflow in semi-arid environments. *Journal* of Arid Environments, 52(2), 245–258. https://doi.org/10.1006/jare. 2001.0947
- Nayak, A., Marks, D., Chandler, D. G., & Seyfried, M. (2010). Long-term snow, climate, and streamflow trends at the reynolds creek experimental watershed, Owyhee Mountains, Idaho, United States. Water Resources Research, 46(6), 1–15. https://doi.org/10.1029/2008WR007525.
- Nolin, A. W., & Daly, C. (2006). Mapping 'at risk' snow in the Pacific northwest. *Journal of Hydrometeorology*, 7(5), 1164–1171. https://doi.org/10.1175/JHM543.1
- Partington, D., Brunner, P., Simmons, C. T., Werner, A. D., Therrien, R., Maier, H. R., & Dandy, G. C. (2012). Evaluation of outputs from automated baseflow separation methods against simulated baseflow from a physically based, surface water-groundwater flow model. *Journal of Hydrology*, 458–459, 28–39. https://doi.org/10.1016/j.jhydrol.2012.06.029
- Payn, R. A., Gooseff, M. N., McGlynn, B. L., Bencala, K. E., & Wondzell, S. M. (2012). Exploring changes in the spatial distribution of stream baseflow generation during a seasonal recession. Water Resources Research, 48(4), 1–15. https://doi.org/10.1029/2011WR011552
- Pellerin, B. A., Wollheim, W. M., Feng, X., & Vörösmarty, C. J. (2008). The application of eletrical conductivity as a tracer for hydrograph separation in urban catchments. *Hydrological Processes*, 22, 1810–1818. https://doi.org/10.1002/hyp
- Penna, D., Engel, M., Mao, L., Dell'agnese, A., Bertoldi, G., & Comiti, F. (2014). Tracer-based analysis of spatial and temporal variations of water sources in a glacierized catchment. *Hydrology and Earth System Sciences*, 18(12), 5271–5288. https://doi.org/10.5194/hess-18-5271-2014
- Pierson, F. B., Slaughter, C. W., & Cram, Z. K. (2000). Monitoring discharge and suspended sediment, Reynolds Creek experimental watershed, Idaho, USA. ARS Technical Bulletin NWRC (September).
- Plummer, L., Busenberg, E., & Cook, P. (2006). Use of chlorofluorocarbons in hydrology. International Atomic Energy Agency.
- Prancevic, J. P., & Kirchner, J. W. (2019). Topographic controls on the extension and retraction of flowing streams. *Geophysical Research Letters*, 46(4), 2084–2092. https://doi.org/10.1029/2018GL081799
- Price, K. (2011). Effects of watershed topography, soils, land use, and climate on baseflow hydrology in humid regions: A review. Progress in Physical Geography, 35(4), 465–492. https://doi.org/10.1177/0309133311402714
- Queener, N. (2015). Spatial and temporal variability in baseflow and stream drying in the Mattole River headwaters. Humboldt State University. https://doi.org/10.1007/springerreference_226434

- Rademacher, L. K., Clark, J. F., Hudson, G. B., Erman, D. C., & Erman, N. A. (2001). Chemical evolution of shallow groundwater as recorded by springs, Sagehen basin; Nevada County, California. *Chemical Geology*, 179(1-4), 37-51. https://doi.org/10.1016/S0009-2541(01)00314-X
- Radke, A. G., Godsey, S. E., Lohse, K. A., McCorkle, E. P., Perdrial, J., Seyfried, M. S., & Holbrook, W. S. (2019). Spatiotemporal heterogeneity of water flowpaths controls dissolved organic carbon sourcing in a snow-dominated, headwater catchment. Frontiers in Ecology and Evolution, 7, 1–23. https://doi.org/10.3389/fevo.2019.00046
- Rumsey, C. A., Miller, M. P., Susong, D. D., Tillman, F. D., & Anning, D. W. (2015). Regional scale estimates of baseflow and factors influencing baseflow in the upper Colorado River basin. *Journal of Hydrology: Regional Studies*, 4, 91–107. https://doi.org/10.1016/j.ejrh.2015.04.008
- Saraiva Okello, A. M. L., Uhlenbrook, S., Jewitt, G. P. W., Masih, I., Riddell, E. S., & Van der Zaag, P. (2018). Hydrograph separation using tracers and digital filters to quantify runoff components in a semi-arid mesoscale catchment. *Hydrological Processes*, 32(10), 1334–1350. https://doi.org/10.1002/hyp.11491
- Schwanghart, W., & Scherler, D. (2014). Short communication: TopoToolbox 2-MATLAB-based software for topographic analysis and modeling in earth surface sciences. Earth Surface Dynamics, 2(1), 1–7. https://doi.org/10.5194/esurf-2-1-2014
- Segura, C., Noone, D., Warren, D., Jones, J. A., Tenny, J., & Ganio, L. M. (2019). Climate, landforms, and geology affect Baseflow sources in a mountain catchment. Water Resources Research, 55(7), 5238–5254. https://doi.org/10.1029/2018WR023551
- Seyfried, M., Lohse, K., Marks, D., Flerchinger, G., Pierson, F., & Holbrook, W. S. (2018). Reynolds Creek experimental watershed and critical zone observatory. *Vadose Zone Journal*, 17(1), 1–20. https://doi.org/10.2136/vzj2018.07.0129
- Sørensen, R., Zinko, U., & Seibert, J. (2006). On the calculation of the topographic wetness index: Evaluation of different methods based on field observations. *Hydrology and Earth System Sciences*, 10(1), 101–112. https://doi.org/10.5194/hess-10-101-2006
- Springer, A. E., & Stevens, L. E. (2009). Spheres of discharge of springs. Hydrogeology Journal, 17(1), 83–93. https://doi.org/10.1007/s10040-008-0341-v
- Tague, C., & Grant, G. E. (2009). Groundwater dynamics mediate low-flow response to global warming in snow-dominated alpine regions. Water Resources Research, 45(7), 1–12. https://doi.org/10.1029/ 2008WR007179
- USGS (2019). Specific conductance: U.S. Geological Survey techniques and methods. In *Book 9, handbooks for water-resources investigations* (pp. 684–684). U.S. Geological Survey. https://doi.org/10.3133/tm9A6.3
- Vega, S. P., Williams, C. J., Brooks, E. S., Pierson, F. B., Strand, E. K., Robichaud, P. R., Brown, R. E., Seyfried, M. S., Lohse, K. A.,

- Glossner, K., Pierce, J. L., & Roehner, C. (2020). Interaction of wind and cold-season hydrologic processes on erosion from complex topography following wildfire in sagebrush steppe. *Earth Surface Processes and Landforms*, 45(4), 841–861. https://doi.org/10.1002/esp.4778
- Ward, A. S., Schmadel, N. M., & Wondzell, S. M. (2018). Simulation of dynamic expansion, contraction, and connectivity in a mountain stream network. Advances in Water Resources, 114, 64–82. https://doi. org/10.1016/j.advwatres.2018.01.018
- Warix, S. R. (2020). Stream drying controls in semi-arid headwater streams: Baseflow, topographic metrics, and diel cycles. Idaho state university.
- Welch, L. A., Allen, D. M., & van Meerveld, H. J. I. (2012). Topographic controls on deep groundwater contributions to mountain headwater streams and sensitivity to available recharge. *Canadian Water Resources Journal*, 37(4), 349–371. https://doi.org/10.4296/cwrj2011-907
- Whiting, J. A., & Godsey, S. E. (2016). Discontinuous headwater stream networks with stable flowheads, Salmon River basin, Idaho. *Hydrologi-cal Processes*, 30(13), 2305–2316. https://doi.org/10.1002/hyp.10790
- Winter, T. C. (2007). The role of ground water in generating streamflow in headwater areas and in maintaining base flow. *Journal of the American Water Resources Association*, 43(1), 15–25. https://doi.org/10.1111/j. 1752-1688.2007.00003.x
- Zimmer, M. A., & McGlynn, B. L. (2017a). Ephemeral and intermittent runoff generation processes in a low relief, highly weathered catchment. *Water Resources Research*, 53(8), 7055–7077. https://doi.org/10.1002/2016WR019742
- Zimmer, M. A., & McGlynn, B. L. (2017b). Bidirectional stream-groundwater flow in response to ephemeral and intermittent streamflow and groundwater seasonality. *Hydrological Processes*, 31 (22), 3871–3880. https://doi.org/10.1002/hyp.11301
- Zimmer, M. A., & McGlynn, B. L. (2018). Lateral, vertical, and longitudinal source area connectivity drive runoff and carbon export across watershed scales. *Water Resources Research*, *54*(3), 1576–1598. https://doi.org/10.1002/2017WR021718

SUPPORTING INFORMATION

Additional supporting information may be found online in the Supporting Information section at the end of this article.

How to cite this article: Warix SR, Godsey SE, Lohse KA, Hale RL. Influence of groundwater and topography on stream drying in semi-arid headwater streams. *Hydrological Processes*. 2021;35:e14185. https://doi.org/10.1002/hyp.14185